Hindawi
Journal of Advanced Transportation
Volume 2018, Article ID 2310905, 15 pages
https://doi.org/10.1155/2018/2310905

Research Article

Modelling Rail-Based Park and Ride with Environmental Constraints in a Multimodal Transport Network

Xinyuan Chen and Inhi Kim

Monash Institute of Transport Studies, Australia

Correspondence should be addressed to Inhi Kim; inhi.kim@monash.edu

Received 3 July 2018; Revised 4 September 2018; Accepted 12 September 2018; Published 4 October 2018

Guest Editor: David Z. W. Wang

Environmental sustainability is a significant aspect in the sustainable development of modern urban cities, especially in the road transport system. As traffic demands increase, public transport requires more promotion to accommodate the increasing travel demands while maintaining the environmental quality. Public transport, however, is less attractive in vast suburb areas mainly due to its longer travel distance and waiting time. Therefore, this paper proposes a rail-based Park-and-Ride (RPR) scheme to promote public transport in the multimodal transport network. To remedy the heterogeneous distribution of vehicle pollutants in the network, regulations in environmental sensitive districts are required and studied in this paper. To quantitatively evaluate and analyse this joint RPR and environmental regulation strategy in multimodal transport systems, this paper develops an environmental constrained combined modal split and traffic assignment (EC-CMSTA) model. The proposed formulation adopts the concept of fix-point to reformulate the nonlinear complementarity conditions associated with the combined modal split and user equilibrium conditions, which is subsequently incorporated into a VI formulated nonlinear complementarity conditions associated with environmental constraints. The proposed VI formulation can handle a general constraint structure, which enhances the modelling adaptability and flexibility. The strictly monotone and Lipschitz continuity properties of this model are rigorously proved, giving rise to efficient algorithms for the model. A customized projection based self-adaptive gradient projection (SAGP) algorithm is then developed. Numerical studies demonstrate that the EC-MSTA model could enhance the behavioural modelling of network users' travel decisions and assist in quantitatively evaluating the effectiveness of RPR schemes and environmental regulations.

1. Introduction

Environmental protection is an important component in the sustainable development of modern urban cities and closely related to the transport system. According to Hong Kong Air Pollutant Emission Inventory (2016), the amount of CO generated in the year of 2016 in Hong Kong is 58600 tones and among them, road transport contributes to 31500 tones and shares 54% of the CO emissions. Also, the US's environmental protection agency reported motorized vehicles in the United States contribute to 86% of CO emissions, 62% of NO_x emissions, 12% of PM2.5 emissions, and 7% of SO_2 emissions [1]. Kitthamkesorn et al. [2] pointed out that only about 20% of the world's town residents enjoy good enough air quality as measured by the levels of emissions and over 600 million people in urban areas worldwide were exposed to dangerous levels of traffic-generated emissions from congestion. In addition, these emissions have not only adverse effects on human health but also a source of greenhouse gas that contributes to global warming [3].

With these adverse effects, the promotion of alternative green transport modes is thus pressing for the governments and transportation authorities to accommodate the growing travel demand while maintaining the environmental quality. Public transport aiming to satisfy the travel demand of urban commuters safely, quickly, and affordably is therefore a significant alternative to private transport. However, in vast suburb areas which are far away from an urban centre, public transport becomes less attractive, mainly due to the unreliable time table, tortuous bus itinerary, much lower travel speed, and lack of door to door services [4]. Large-scale deployments of public transport system in the remote areas are hardly seen

as an economical available strategy. Park and Ride (P&R), therefore, becomes an important strategy to promote public transport since it enables travellers to drive when the road is not congested and to change a mode to transit accessing to CBD without traffic congestion. Since its first implementation in 1930s, P&R has been widely recognized as a significant traffic management strategy and becomes an indispensable part of majority modern urban cities.

P&R can be categorized into bus-based P&R (BPR) and rail-based P&R (RPR) based on its ride component [5]. In a metropolis with advanced rail system, rail-based P&R is superior to bus-based P&R, due to the faster speed, higher level of safety, comfortability, and its advantages in environmental protection (zero-emission).

Despite the fact that environmental deterioration could somehow be alleviated by promoting public transport through RPR schemes, the environmental requirements are usually not strictly met in certain districts mainly due to the heterogeneous distribution of pollution in the network [3]. To remedy this limitation, specific environmental regulations, therefore, are required to certain district, e.g., the city business district (CBD) with many tall buildings, to protect the environmental quality in this area.

Therefore, we aim to use RPR services to assist mode shift to reduce the overall vehicle travel demands in the road network and then apply area-based regulation scheme to deal with the environmental deterioration caused by heterogeneity of traffic flows. The environmental protection approaches are integrated as a combined strategy in this paper. Previous studies revealed that a systematic study is necessary to properly understand and evaluate the effectiveness of the environmental regulations, as well as the RPR scheme. Thus, this paper focuses on the modelling and solution algorithm development of the proposed environmental protection strategy.

2. Literature Review

Road network equilibrium approaches are commonly preferred for estimating vehicle emissions and noises [3], because the distribution of vehicle pollution heavily relies on the states of traffic flows [6]. Other than the overall pollution level, the spatial distribution level should be controlled since it is heterogeneous.

One line of the research developed models by setting environmental protection as objectives [3], modelling environmental considerations as an objective function. Rilett and Benedek [7] proposed the concept of emission optimum (EO) and emission-oriented user equilibrium (EOUE), in which the former one assumes travellers make route choices with the objective of minimizing the total emissions or noises, and the latter includes the toll charges to represent the impact on the environment. Later, Benedek and Rilett [8] made extension by modelling the assignment of vehicles based on equity which considers the objectives of neighbouring residents, rather than the system operator's or drivers' objectives. Sugawara and Niemeier [9] used the emissions-optimized trip assignment model to estimate the maximum carbon monoxide emission reduction under varying congestion levels.

Although the overall environmental quality could somehow be improved by taking the environmental considerations as the objective, the pollution level is not always strictly met on each link and zone in the road network. Therefore, another line of the research focuses on modelling the emission as environmental constraints. Chen, Zhou and Ryu [10] developed a traffic assignment model by considering various physical and environment restrictions as side constraints, which is formulated as a VI problem and solved by a predictor-corrector (PC) algorithm. Li et al. [11] developed a toll design model by simultaneously considering congestion and environmental externalities. Recently, Xu, Chen, and Cheng [1] reformulated the environmental constrained traffic assignment model through a smooth gap function to enhance the modelling adaptability and flexibility.

As a rational extension of traffic assignment problem, Nagurney, Ramanujam, and Dhanda [12] extended the environmental constrained traffic assignment problem to the case of multimodal traffic network. However, the model presented in this paper simply follow the deterministic user equilibrium (DUE) principle for both modal split and traffic assignment. In order to evaluate the environmental regulation strategy in the multimodal transport network, a better behavioural model is needed. Therefore, the combined modal split and traffic assignment model (CMSTA) is adopted in this paper. In the literature, the CMSTA problems are widely adopted to evaluate the P&R schemes. Fernandez et al. [13] conducted an initial work to model P&R in deterministic case. Later, this work was extended to the case of asymmetric link travel time functions by García and Marín [14] and to the logit-based stochastic model by Li et al. [15] and Lam et al. [16]. Recently, Liu and Meng [5] provided a formulation for the bus-based P&R in a network with the congestion charge. Pineda et al. [17] and Song, He, and Zhang [18] developed an integrated P&R facilities and transit service optimization model. Kitthamkesorn et al. [2] and Kitthamkesorn and Chen [19] considered the influence of "go green" transport modes on environmental protection by taking use of recent advances in logit model. Liu et al. [20] proposed a new concept of P&R, remote park and ride, and developed an exact solution method for the optimal design of parking facilities, following the nonlinear valid inequality technique [21, 22]. Some other studies focus on the P&R schemes in a linear corridor, e.g., Liu et al. [23], Wang and Du [24], and Du and Wang [25]. However, these studies mainly focus on congestion alleviation. As abovementioned, the environmental requirements in certain areas are not considered. Therefore, a more general modelling framework that incorporates environmental requirements is needed. To this end, this paper aims to build an environmental constrained combined modal split and traffic assignment (EC-CMSTA) model to better evaluate and analyse environmental sustainable transportation development strategies.

This paper distinguishes itself from previous studies in threefold aspects. First, we propose EC-CMSTA, CMSTA model with side constraints, which could handle the general environmental constraint structures, including linear or nonlinear, link based, or area-based constraints. Also, the general link/route cost structure is considered here. Second, by incorporating general side constraints into CMSTA, solving is much more complex compared to the traditional side constrained unimodal traffic equilibrium problems. To explicitly

consider the general environmental constraints and make use of existing efficient algorithms, we propose a VI formulation by adapting the concept of fix-point. This VI formulation is strictly monotone and Lipschitz continuous, permitting a number of existing efficient algorithms for its solution [10, 26]. Third, even though the solution methods for the traffic assignment problems with side constraints have been well studied with numerous achievements [1, 10, 12, 27], solutions for the multimodal traffic equilibrium with side constraints are relatively limited. Recently, Meng, Liu and Wang [28] proposed a CA incorporated self-adaptive PC algorithms to solve asymmetric stochastic user equilibrium (SUE) problem with elastic demand and link capacity constraints. Inspired by Meng, Liu, and Wang [28], we extend this approach to multimodal traffic equilibrium problem and develop a customized projection based algorithm with a self-adaptive step size scheme which permits the convergence under a much milder assumption of the underlying mapping.

The remainder of this paper is organized as follows: we present assumptions and an EC-CMSTA model for the environmental regulations in the multimodal transport system with RPR scheme in the next section. A general VI formulation and a projection based solution algorithm are provided in Sections 3 and 4. Section 5 provides two numerical studies to validate the proposed methodology. Finally, Section 6 concludes this study.

3. Problem Description

Considering a specific environmental regulation strategy, to analyse its impact in the multimodal transport system, we build a model for the equilibrium flows following environmental requirements.

Given a multimodal transportation network represented by a strongly connected topology graph $G(N, A)$ where N is the set of nodes and A is the set of links. The origins, destinations, and RPR facilities are scattered in the network and represented by certain nodes, $n \in N$. The set of links A can be further categorized into three subsets: set of autolinks A^a; set of rail links A^r; and set of P&R links A^p; $A = A^a \cup A^r \cup A^p$.

3.1. Modelling Environmental Requirements. As abovementioned, the environmental requirements are not strictly met in the road network. Thus, it is necessary to explicit considering environmental protection thresholds to prevent environmental deterioration in certain zones. In the literature, the environmental constraints can be expressed into a general form:

$$g_e(\mathbf{v}) \le 0, \quad \forall e \in E \tag{1}$$

where e is a component of E and E represents a set of environmental sensitivity elements. In the case of link based environmental protection strategy, e represents a link which is assumed in this paper. $\mathbf{v}$ is the vector of link flows; $g_e(\mathbf{v})$ is a function to measure the amount of vehicle pollution and environmental thresholds. Equations (1) ensure the amount of pollution no larger than predetermined thresholds. Note that (1) are general formulation that could measure different types of vehicle pollutants [1]. Herein, we make assumption as follows.

Assumption 1. The environmental threshold measure function $g_e(\mathbf{v}), \forall e \in E$, is a continuously differentiable and strictly monotone increasing function of the link flows $\mathbf{v}$.

Suppose the total number of environmentally sensitive areas in the network is I. The inbound flows of these areas should be restricted according to environmental protection strategies. All the links in the area $i \in I$ are grouped into set E_i, where $E_i \in A$. Then, the specific link based environmental constraints in these areas could be expressed as

$$g_a(\mathbf{v}) \cdot v_a \le \overline{g}_a, \quad \forall a \in E_i,\ i \in I \tag{2}$$

where $g_a(\mathbf{v})$ is the amount of vehicle pollutants per vehicle on link a and $\overline{g}_a$ is the environmental protection threshold on link a imposed by the operators.

3.2. Network Assessment. Due to the fact that the travel decisions of a network user consist of modal choice and route choice, a combined modal split and traffic assignment model is needed. The travel impedance on an auto or rail link is clearly influenced by its flows. For the RPR links, each of them always connects an autolink and a rail link, so that the RPR flows could transfer. The total travel impedance on a RPR link includes the time spent on parking, waiting/boarding the dedicated bus as well as the bus in-vehicle travel time, which is clearly flow-dependent. We then make the following assumption.

Assumption 2. The link travel time $t_a(\mathbf{v}), a \in A$ is a continuously differentiable, monotone increasing of the link flow $\mathbf{v}$.

Let K_m^{od} denote the set of paths under m; $f_k^{m,od}$ denotes the flow on path $k \in K_m^{od}$ for mode m; q_m^{od} denotes the demand of mode m; and $\overline{q}^{od}$ denotes the total travel demand between OD pair (o, d). We have the following flow conservation conditions:

$$\sum_{m \in M_{od}} q_m^{od} = \overline{q}^{od}, \quad \forall od \in W \tag{3}$$

$$q_m^{od} \ge 0, \quad \forall m \in M_{od},\ od \in W \tag{4}$$

$$\sum_{k \in K_m^{od}} f_k^{m,od} = q_m^{od}, \quad \forall m \in M_{od},\ od \in W \tag{5}$$

$$f_k^{m,od} \ge 0, \quad \forall k \in K_m^{od},\ m \in M_{od},\ od \in W \tag{6}$$

$$v_a = \sum_{od \in W} \sum_{m \in M_{od}} \sum_{k \in K_m^{od}} f_k^{m,od} \delta_{a,k}^{m,od}, \quad \forall a \in A \tag{7}$$

where (3) and (5) define demand/flow conservation conditions. Equations (4) and (6) are the nonnegativities. Equations (7) define the link-path flow relationship. Constraints (1), (3)-(7) define the feasible set of Ω of $(\mathbf{v}, \mathbf{f}, \mathbf{q})$ where $\mathbf{v} := (v_a, a \in A)$ is the vector of link flows; $\mathbf{f} := (f_k^{em,od}, k \in K_m^{od}, m \in M^{od}, od \in W)$ is the vector of path flows; and $\mathbf{q} := (q_m^{od}, m \in M^{od}, od \in W)$ is the vector of modal demands.

Let W denote the set of OD pairs; $\overline{q}^{od}$ denote the total travel demand for $(o,d) \in W$; and M_{od} denote the set of modes between OD pair (o,d). The multinomial logit (MNL) model is adopted to analyse the modal split pattern. The probability of choosing any mode m between an OD pair (o,d) equals

$$p_m^{od} = \frac{\exp\left(-\theta \cdot \tau_m^{od}\right)}{\sum_{i \in M_{od}} \exp\left(-\theta \cdot \tau_i^{od}\right)}, \quad \forall m \in M,\ od \in W \tag{8}$$

where $\theta \in [0, +\infty)$ is the dispersion parameter and τ_m^{od} is the deterministic component of the utility of mode m between OD pair (o,d), which can be taken as the equilibrium path travel time of mode m. The satisfaction of MNL, $S_{od}(\tau_m^{od})$, equals $\tau_m^{od} + (1/\theta)\ln(q_m^{od})$, which is concave function [28].

The user equilibrium path flow solution is then formulated by the following conditions:

$$f_k^{m,od}\left(c_k^{m,od} - \varphi_m^{od}\right) = 0, \quad \forall k \in K_m^{od},\ m \in M_{od},\ od \in W \tag{9}$$

$$f_k^{m,od} \geq 0, \quad \left(c_k^{m,od} - \varphi_m^{od}\right) \geq 0, \quad \forall k \in K_m^{od},\ m \in M_{od},\ od \in W \tag{10}$$

where φ_m^{od} is the Lagrange multiplier associated with the constraints (5), which represents the travel impedance of using mode m. At equilibrium, the travel time $c_k^{m,od}$ of a used path $k \in K_m^{od}$ equals φ_m^{od}. All commuters under mode m have identical path travel time, and no traveller can unilaterally reduce his/her travel time by changing routes.

4. Variational Inequality Formulation

In this section, we propose two equivalent VI formulations for the proposed EC-CMSTA model. In order to strengthen the flexibility and adaptability of the proposed model, we further make the following two assumptions.

Assumption 3. The link travel time function is asymmetric, i.e., t_a is not only affected by its own flow v_a, but also flows on some other links, which is expressed as $t_a = t_a(\mathbf{v})$.

Assumption 4. The path travel time c_k is nonadditive to its links, i.e., $c_k \neq \sum_a t_a \delta_{a,k}$, where $\delta_{a,k} = 1$ if path k uses link $a \in A$ and 0 otherwise.

Then, the VI mode for EC-CMSTA is formulated as follows:

$$\sum_{od \in W} \sum_{m \in M_{od}} \sum_{k \in K_m^{od}} c_k^{m,od}\left(\mathbf{f}^*, \mathbf{q}^*\right)\left(f_k^{m,od} - f_k^{m,od*}\right) + \sum_{od \in W} \sum_{m \in M_{od}} \tilde{c}_m^{od}\left(\mathbf{f}^*, \mathbf{q}^*\right)\left(q_m^{od} - q_m^{od*}\right) \geq 0, \quad \forall \left(\mathbf{f}^*, \mathbf{q}^*\right) \in \Omega \tag{11}$$

where $c_k^{m,od}$ is the travel time on route k, where $k \in K_m^{od}$. $\tilde{c}_m^{od} = (1/\theta)\ln(q_m^{od})$ represents the entropy term in travel cost function of mode m, $m \in M_{od}$; $f_k^{m,od*}$ and q_m^{od*} are the optimal solution of this problem; $\mathbf{f}^*$ and $\mathbf{q}^*$ are the vector of optimal solution.

Let $\mathbf{c}$ be the vector of $c_k^{m,od}$ and $\tilde{\boldsymbol{\tau}}$ be the vector of $\tilde{c}_m^{od}$, i.e., $\mathbf{c} := (c_k^{m,od},\ k \in K_m^{od},\ m \in M_{od},\ od \in W)^T$ and $\tilde{\boldsymbol{\tau}} := (\tilde{c}_m^{od},\ m \in M_{od},\ od \in W)^T$. The VI formulation can be simplified as

$$\mathbf{c}\left(\mathbf{f}^*, \mathbf{q}^*\right)^T\left(\mathbf{f} - \mathbf{f}^*\right) + \tilde{\boldsymbol{\tau}}\left(\mathbf{f}^*, \mathbf{q}^*\right)^T\left(\mathbf{q} - \mathbf{q}^*\right) \geq 0, \quad \forall \left(\mathbf{f}^*, \mathbf{q}^*\right) \in \Omega \tag{12}$$

Note that the inclusion of nonlinear environmental constraints makes the feasible set more complex in general. Existing solution algorithms for CMSTA cannot be directly adopted to solve it. Most of existing studies focus on solving the simplified linear link capacity constrained traffic equilibrium problems by a penalty based algorithm. However, due to the complexity of EC-CMSTA (simultaneous achieving equilibrium for both route flow and modal demand), reformulating it into an integrated formulation or directly solving it by a penalty/gradient based algorithm is less effective. Therefore, this paper develops an alternative approach to reformulate the EC-CMSTA which permits existing solution algorithms for its solution.

4.1. Alternative VI Formulation. Daganzo [29] built a fix-point model in terms of link flows for the asymmetric SUE problem with fixed demand and showed availability of the MSA, which was extended by Cantarella [30] to the case of asymmetric SUE problem with elastic demand. Recently, Meng, Liu and Wang [28] further made extension by incorporating link capacity constraints. This problem was formulated as a VI problem by incorporating the fix-point formulated asymmetric SUE problem with elastic demand. Following the same technique, we propose a fixed point reformulated CMSTA model which is expressed as follows:

$$v_a = \sum_{od \in W} \overline{q}^{od} \sum_{m \in M_{od}} p_m^{od}\left(\mathbf{f}\left(\mathbf{v}\right)\right) \times P_a^{m,od}\left(\mathbf{f}\left(\mathbf{v}\right)\right), \quad \forall a \in A \tag{13}$$

where $\mathbf{v}$ is the equilibrium link flow solution, p_m^{od} is the probability of mode choice defined in (8), and $P_a^{m,od}$ is the link usage probability defined by

$$P_a^{m,od}\left(\mathbf{f}\left(\mathbf{v}\right)\right) = \sum_{k \in K_m^{od}} p_k^{m,od}\left(\mathbf{f}\left(\mathbf{v}\right)\right) \delta_{k,a}^{m,od}, \quad \forall a \in A \tag{14}$$

and $p_k^{m,od}$ is the probability of path k perceived as the shortest one among the path set K_m^{od}. In the deterministic case, $p_k^{m,od}$ equals one if path k is the shortest path among alternatives and zero otherwise.

A set of generalized SUE conditions with elastic demand and capacity constraints was proposed by Meng, Liu, and Wang [28] for the optimal solution of SUE problem with elastic demand, asymmetric link travel time function and link capacity constraints. These conditions can be further

extended to the multimodal transport system which is the problem addressed in this paper. Let $\mathbf{v}$ denote the equilibrium link flow pattern of the addressed problem if and only if there exists a vector of Lagrangian multipliers corresponding to environmental constraints, denoted by $\mathbf{u}^* = (u_e^*, e \in E)^T$.

$$v_a(\mathbf{u}) = \sum_{od \in W} \sum_{m \in M_{od}} q_m^{od}(\mathbf{f}(\mathbf{v}), \boldsymbol{\lambda}(\mathbf{u}^*)) \times P_a^{m,od}(\mathbf{f}(\mathbf{v}), \boldsymbol{\lambda}(\mathbf{u}^*)), \quad \forall a \in A \tag{15}$$

$$-g_e(\mathbf{v}) \geq 0, \quad \forall e \in E \tag{16}$$

$$u_e^* \cdot (-g_e(\mathbf{v})) = 0, \quad \forall e \in E \tag{17}$$

$$u_e^* \geq 0, \quad \forall e \in E \tag{18}$$

where $\boldsymbol{\lambda}(\mathbf{u}^*)$ is defined by

$$\boldsymbol{\lambda}(\mathbf{u}^*) = \left(\lambda_k^{m,od} = \sum_{e \in E} u_e^* \zeta_{e,k}^{m,od}, \ \forall k \in K_m^{od}, \ m \in M_{od}, \ od \in W \right)^T \tag{19}$$

and $\zeta_{e,k}^{m,od} = 1$ if path $k \in K_m^{od}$ goes through $e \in E$ and $\zeta_{e,k}^{m,od} = 0$, otherwise. Based on the optimal Lagrangian multiplier $\mathbf{u}^*$, the EC-CMSTA is identical to the CMSTA in terms of generalized link travel time functions.

$$\hat{t}_a(\mathbf{v}, \mathbf{u}^*) = \begin{cases} t_a(\mathbf{v}) + u_a^*, & \forall a \in E \\ t_a(\mathbf{v}), & \forall a \in A/E \end{cases} \tag{20}$$

Equations (16)-(18) imply that if there is no environmental constraint on any link $a \in E$, $u_a^* = 0$.

Note that the complementary slackness conditions (see (16)-(18)) could be regarded as a nonlinear complementary problem (NCP) of the vector of Lagrangian multipliers $\mathbf{u}^*$. Due to the feasible set of $\mathbf{u}$ is defined on the whole nonnegative orthant, this NCP problem can be equivalently formulated as a VI model. Hence, the alternative formulation of VI (11) is proposed as follows:

$$\mathbf{g}(\mathbf{u}^*)^T (\mathbf{u} - \mathbf{u}^*) \geq 0, \quad \forall \mathbf{u} \in \mathfrak{R}_+^{|E|} \tag{21}$$

where $\mathfrak{R}_+^{|E|} = (u_e \geq 0, e \in E)^T$ denotes the feasible set. $\mathbf{g}(\mathbf{u})$ is the $|E|$ dimensional vector functions, which measures vehicle pollution:

$$\mathbf{g}(\mathbf{u}) = (-g_e(\mathbf{v}(\mathbf{u})), \ \forall e \in E)^T : \mathfrak{R}_+^{|E|} \longrightarrow \mathfrak{R}^{|E|} \tag{22}$$

$\mathbf{g}(\mathbf{u}^*)$ is thus the optimal solution of the VI problem (21). Herein, $\mathbf{v}(\mathbf{u})$ is a link flow solution for the CMSTA with the generalized link travel time functions (20) (without environmental constraints). In other words, $\mathbf{v}(\mathbf{u})$ is a solution of the fix-point model with the Lagrangian multiplier $\mathbf{u}$:

$$v_a(\mathbf{u}) = \sum_{od \in W} \sum_{m \in M_{od}} q_m^{od}(\hat{\mathbf{t}}(\mathbf{v}, \mathbf{u})) \times P_a^{m,od}(\hat{\mathbf{t}}(\mathbf{v}, \mathbf{u})), \quad \forall a \in A \tag{23}$$

where $\hat{\mathbf{t}}(\mathbf{v}, \mathbf{u}) = (\hat{t}_a(\mathbf{v}, \mathbf{u}), \ \forall a \in A)$ denotes the vector of generalized link travel time functions.

Note that the feasible set $\mathfrak{R}_+^{|E|}$ of $VI(\mathbf{g}, \mathfrak{R}_+^{|E|})$ is unbounded, which makes it difficult to shown the existence of a solution to VI model $VI(\mathbf{g}, \mathfrak{R}_+^{|E|})$. Fortunately, according to Meng, Liu and Wang [28], one can always find an upper bound $\overline{M}$ for $u_a, \forall a \in E$. Therefore, we define a subset $\overline{\Omega}$ of $\mathfrak{R}_+^{|E|}$ which is bounded by $\overline{M}$. The restricted VI model is subsequently formulated as

$$\mathbf{g}(\mathbf{u}^*)^T (\mathbf{u} - \mathbf{u}^*) \geq 0, \quad \forall \mathbf{u} \in \overline{\Omega} \tag{24}$$

The feasible set $\overline{\Omega}$ is a nonempty, closed, and convex set. To show the existence of solution to $VI(\mathbf{g}, \overline{\Omega})$ as well as the convergence of its solution algorithm, the following properties of vector function $\mathbf{g}(\mathbf{u})$ are proposed. Rigorous proofs of Propositions 5 and 6 are given in the Appendices A and B, respectively.

Proposition 5. *Vector function* $\mathbf{g}(\mathbf{u})$ *is strictly monotone on* $\overline{\Omega}$*; namely,*

$$(\mathbf{g}(\mathbf{u}') - \mathbf{g}(\mathbf{u}''))^T (\mathbf{u}' - \mathbf{u}'') > 0, \quad \forall \mathbf{u}', \mathbf{u}'' \in \overline{\Omega} \tag{25}$$

Proposition 6. *Vector function* $\mathbf{g}(\mathbf{u})$ *is Lipschitz continuous on* $\overline{\Omega}$*; namely,*

$$\|\mathbf{g}(\mathbf{u}') - \mathbf{g}(\mathbf{u}'')\|_2 \leq L \|\mathbf{u}' - \mathbf{u}''\|, \quad \forall \mathbf{u}', \mathbf{u}'' \in \overline{\Omega} \tag{26}$$

Though we have Propositions 5 and 6, the existence of a solution to VI model $VI(\mathbf{g}, \overline{\Omega})$ can be ensured. We proceed to prove the equivalence between the VI model $VI(\mathbf{g}, \overline{\Omega})$ and the generalized CMSTA conditions and summarized in Proposition 7. Rigorous proofs are given in Appendix C.

Proposition 7. $\mathbf{u}^* = (u_a^*, \ \forall a \in E)$ *is a solution of* $VI(\mathbf{g}, \overline{\Omega})$ *if and only if* $\mathbf{u}^*$ *and* $\mathbf{v}(\mathbf{u}^*)$ *fulfil the generalized CMSTA conditions (15)-(18).*

5. Solution Algorithm

As the vector function $\mathbf{g}(\mathbf{u})$ of the VI model $VI(\mathbf{g}, \overline{\Omega})$ is an implicit function, it is burdensome to directly evaluate its gradient. On the other hand, with any given Lagrangian multiplier vector $\mathbf{u}$, the value of vector function $\mathbf{g}(\mathbf{u})$ can be evaluated by solving the CMSTA with generalized travel time with no constraints, which can be efficiently solved by a number of existing solution algorithms.

Projection type algorithms have been thoroughly studied and proven to be efficient in solving traffic equilibrium problems [31–33]. Among them, the gradient projection (GP) is commonly adopted due to its concise form and good performance, for which a recent survey can be found in Ryu, Chen, and Choi [34]. The self-adaptive gradient projection (SAGP) algorithm was originally proposed by He et al. [35], where the gradient projection operation is adopted to establish the descent direction, coupled with a self-adaptive step size scheme to permit the convergence under a much milder assumption of the underlying mapping, and thus can handle general cost mapping structures and generalized side

constraints. Later, Han and Sun [36] adopted this method to solve the asymmetric traffic assignment problems. Chen, Zhou, and Xu [32] further used this method to solve the asymmetric traffic assignment problem with nonadditive route cost functions. Inspired by previous studies, this paper presents the SAGP algorithm specifically designed for solving the CMSTA with generalized travel time functions.

As for the Lagrangian multipliers $\mathbf{u}$, the projection operation on Ω of the VI model $VI(\mathbf{g}, \overline{\Omega})$ is straightforward, as well. Propositions 5 and 6 imply the monotony and continuity of the VI model $VI(\mathbf{g}, \overline{\Omega})$. Therefore, the projection based algorithm is also suitable to evaluate the Lagrangian multipliers solutions. To this end, this section proposes a nested SAGP algorithm to solve the EC-CMSTA model which is presented as follows.

Step 0 (initiation). Set parameters of SAGP within the given range: $\delta \in (0,1)$, $\mu \in [0.5,1]$, $\varepsilon > 0$, $\alpha_{\max} > 0$, $\alpha^{(0)} > 0$, $\gamma^{(0)} = \alpha^{(0)}$. Set the iteration counter: $n = 0$, and the initial solution which should be a feasible solution: $\mathbf{u}^{(0)} = (u_a^{(0)} = 0, a \in E)^T$.

Step 1 (self-adaptive scaling procedure). This step aims to find the largest step size $\alpha^{(n+1)}$ that satisfies the given criteria in (27). To this end, let $\alpha^{(n+1)} = \mu^{l^{(n)}}\gamma^{(n)}$, and set nonnegative integer $l^{(n)} = 0$. We perform the following procedures, if the given criterion is satisfied, terminate and go to Step 2; otherwise, let $l^{(n)} = l^{(n)} + 1$, and perform the following procedures again.

Step 1.1. Given vector $\mathbf{u}^{(n)}$, evaluate the CMSTA with generalized travel time functions (23), using SAGP algorithm, and obtain the equilibrium flows $(\mathbf{v}^{(n)}, \mathbf{q}^{(n)})$. The solutions are subsequently used to evaluate the environmental measurement function $\mathbf{g}(\mathbf{u}^{(n)})$.

Step 1.2. Perform the projection operation for $\mathbf{u}^{(n)}$ to obtain a tentative vector $\tilde{\mathbf{u}}^{(n+1)}$, i.e., $\tilde{\mathbf{u}}^{(n+1)} = P_\Omega[\mathbf{u}^{(n)} - \alpha^{(n+1)} \cdot \mathbf{g}(\mathbf{u}^{(n)})]$.

Step 1.3. Let $\overline{\mathbf{u}}^{(n+1)} = \max[0, \mathbf{u}^{(n)} - \alpha^{(n)}\mathbf{g}(\mathbf{u}^{(n)})]$. If the following inequality is satisfied

$$\begin{aligned}&(2-\delta)\,\alpha^{(n+1)}\left(\mathbf{u}^{(n)} - \tilde{\mathbf{u}}^{(n+1)}\right)^T\left(\mathbf{g}\left(\mathbf{u}^{(n)}\right) - \mathbf{g}\left(\tilde{\mathbf{u}}^{(n+1)}\right)\right)\\ &\quad + \left(\alpha^{(n+1)}\right)^2\left\|\mathbf{g}\left(\mathbf{u}^{(n)}\right) - \mathbf{g}\left(\tilde{\mathbf{u}}^{(n+1)}\right)\right\|^2\\ &\geq \max\left\{0, \frac{\left(\alpha^{(n+1)}\right)^2 - \left(\alpha^{(n)}\right)^2}{\left(\alpha^{(n)}\right)^2}\left\|\mathbf{u}^{(n)} - \overline{\mathbf{u}}^{(n+1)}\right\|^2\right\}\end{aligned} \tag{27}$$

go Step 2. Otherwise, let $l^{(n)} = l^{(n)} + 1$, update step size $\alpha^{(n+1)}$, and go back to Step 1.1.

Step 2 (selection of $\gamma^{(n+1)}$). If the following condition is satisfied, let $\gamma^{(n+1)} = \max\{\alpha^{(n+1)}/\mu, \alpha_{\max}\}$.

$$\begin{aligned}&0.5\alpha^{(n+1)}\left(\mathbf{u}^{(n)} - \tilde{\mathbf{u}}^{(n+1)}\right)^T\left(\mathbf{g}\left(\mathbf{u}^{(n)}\right) - \mathbf{g}\left(\tilde{\mathbf{u}}^{(n+1)}\right)\right)\\ &\quad + \left(\alpha^{(n+1)}\right)^2\left\|\mathbf{g}\left(\mathbf{u}^{(n)}\right) - \mathbf{g}\left(\tilde{\mathbf{u}}^{(n+1)}\right)\right\|^2\\ &\geq \max\left\{0, \frac{\left(\alpha^{(n+1)}\right)^2 - \left(\alpha^{(n)}\right)^2}{\left(\alpha^{(n)}\right)^2}\left\|\mathbf{u}^{(n)} - \overline{\mathbf{u}}^{(n+1)}\right\|^2\right\}\end{aligned} \tag{28}$$

Step 3 (convergence test). If the convergence criterion is satisfied, terminate; otherwise, let iteration counter: $n = n+1$, go back to Step 1.

Note that the CMSTA with generalized travel time functions in Step 1.1 is also solved by the SAGP algorithm, which is not repeated here for conciseness.

6. Numerical Examples

In this section, two experiments based on a linear network and the Sioux-Falls network are provided to demonstrate the features of the proposed EC-CMSTA and validity of the proposed solution algorithm.

It is well known that carbon monoxide (CO), carbon dioxide (CO_2), sulphur dioxide (SO_2), nitrogen oxides (NO_x), respirable suspended particulates (RSP or PM_{10}), fine suspended particulates (FSP or $PM_{2.5}$), and volatile organic compounds (VOC) are the main types of vehicular emission pollutants that are critical for air quality protection. Among others, CO is taken as an important indicator of the level of vehicle atmosphere pollution, mainly because (1) vehicles contribute to the majority of CO emissions in the atmosphere; (2) CO is one of the most critical pollutants among the various types of vehicular emissions; (3) the emission functions of other pollutants are similar to that of CO [11]. In addition, this consideration has also been used in a number of recent studies, e.g., Yin and Lawphongpanich [37]; Nagurney, Qiang and Nagurney [38]; Chen, Zhou and Ryu [10]; Li et al. [11]; Xu, Chen and Cheng [1]; Yang, Ban and Ma [39]; Kitthamkesorn et al. [2]. Therefore, we use CO as an illustration to model vehicle emission. The nonlinear macroscopic formula of CO emission rate proposed by Wallace et al. [6] is used for analysis as shown below:

$$g_a(t_a) = 0.2038 \cdot t_a \cdot \exp\left(\frac{0.7962 \cdot L_a}{t_a}\right) \tag{29}$$

where $g_a(t_a)$ is the CO emission rate on link a measured in grams per hour. L_a is the length of link a measured in kilometers, and t_a is the link travel time measured in minutes. This nonlinear function can be shown to be convex and continuously differentiable. The Bureau of Public Road (BPR) type function is adopted for the link travel time, i.e., $t_a = t_a^0(1+0.15(v_a/C_a)^4)$ for road links, and $t_a = t_a^0(1+0.1(v_a/C_a)^4)$ for rail and RPR links. The dispersion parameter of MNL mode is set as $\theta = 1.0$.

6.1. A Linear Corridor. As shown in Figure 1, consider a linear corridor $G(N, A)$, with one rail line (dotted line) from suburb o to the urban city area d and another highway (solid line)

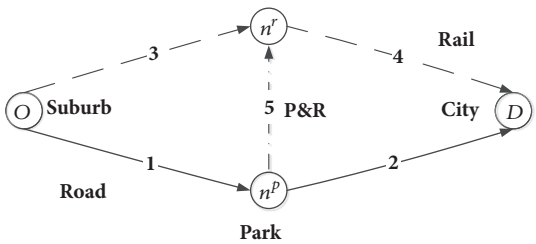

Figure 1: A linear corridor with RPR facility.

Table 1: Attributes of the linear corridor.

Link Type	Auto		Rail		RPR
Link No.	1	2	3	4	5
Free Flow Travel Time (t_a^0)	6	4	12	5	3
Capacity (C_a)	250	200	350	350	350

Table 2: Modal share and equilibrium travel time.

Modes	With RPR scheme	
	Demand	Travel time
Auto	250.45	16.66
Train	150.15	17.16
RPR	99.38	17.58

connecting (o, d). The OD demand is assumed to be 500 per hour. One RPR site is constructed at n^p, adjacent to the train station n^r. Travellers transfer from the RPR site n^p to the train station n^r through the RPR link (link 5). Link 2 passes into an environmentally sensitive urban area, which exerts restriction on the total CO emissions on link 2. Using the CO emission rate function defined by (29), the nonlinear environmental constraint on link a can be expressed as

$$0.2038 \cdot t_a \cdot \exp\left(\frac{0.7962 L_a}{t_a}\right) \cdot v_a - \overline{g}_a \leq 0, \quad \forall a \in A \quad (30)$$

where $\overline{g}_a$ is the CO emission threshold on link a. Attributes of the network are given in Table 1.

Setting the environmental constraints at 500, we first examine the correctness of the results. As expected, the results in Table 2 satisfy the modal demand conversation condition and the MNL based modal choice condition. The Lagrangian multiplier on link 2 equals 1.73, permitting the emission on link 2 subject to the requirements.

We proceed to explore the influence of the environmental constraint on the flow shift of modal demands, link flows, and total system travel time by varying the emission constraint $\overline{g}_2$ between 0 and 800. The corresponding modal demand shift pattern under environmental constraint is given in Figure 2. We can see that as $\overline{g}_2$ increases (relax the CO emission constraints), the auto demand first increases and then becomes stable; meanwhile, the demands of rail and RPR show the crosscurrent. It makes sense because relaxing $\overline{g}_2$ is similar to increase the road capacity. When the emission level is beyond 631.47, constraint (30) is not blinding anymore which means the PRP facilities are able to achieve the environmental

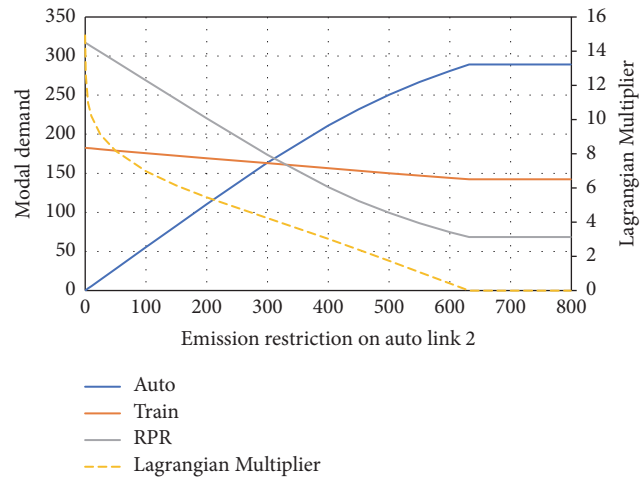

Figure 2: Modal split pattern with various environmental constraint level.

protection requirements without additional regulations or restrictions. The dotted line indicates the evolution of Lagrangian multiplier on link 2, u_2^*. As the environmental regulation can be strengthened, u_2^* keeps increasing and trends to be infinity, when $\overline{g}_2 = 0$.

Detailed results of link flows, link travel time, and Lagrangian multiplier are shown in Table 3. As marked by bold and italic text in Table 3 the minimal system travel cost is achieved when $\overline{g}_2$ is increased to around 631.47. In other words, setting $\overline{g}_2 \geq 631.47$ is equivalent to have no CO emission constraint on link 2, which reduces the problem into CMSTA. Meanwhile, the Lagrangian multiplier u_2^* reduces to zero as well indicating that there is no restrictions for vehicles which come into this area.

6.2. Sioux-Falls Network. Another numerical example built from the Sioux-Falls network (Figure 3) is used to further access the performance of the proposed model and solution algorithm for solving the environmental constrained CMSTA problem. This study network consists of 30 nodes and 76 links. The area highlighted by the red ellipse is the CBD district. It has four rail lines between the suburb areas and the city loop. Detail attributes of this network are tabulated in Appendix D. We focus on the travel demands in commuting hours, where the majority of travel demands origin from the suburbs and go into business districts. There are 24 OD pairs and the OD demand data are given in Appendix E. Four sites (nodes 3, 6, 19, and 14) which locate close to rail lines are selected as RPR car parks where RPR users park their car and transfer to rail mode.

The column generation scheme is adopted in this case and incorporated into our proposed solution algorithm to generate paths in evaluating the equilibrium flows. In the multimodal transport network, we first examine the effect of the proposed RPR scheme with the CMSTA model and access the emissions in the road subnetwork. 5 links in the CBD district are subsequently identified as the critical links, and be further grouped into the link set $\overline{A} = \{14, 22, 29, 46, 48\}$. As shown in Figure 4, the provision of RPR facilities significantly

Table 3: Link flows and link cost with varied restricted CO emission level.

$\overline{g}_2$	Link 1		Link 2			Link 3		Link 4		Link 5	
	Time	Flow	Time	Flow	u^*	Time	Flow	Time	Flow	Time	Flow
0	8.33	317.29	4.00	0.00	$+\infty$	12.09	182.71	7.08	499.94	3.20	317.23
100	8.55	324.24	4.00	55.32	6.99	12.08	175.76	6.30	444.68	3.10	268.92
200	8.76	330.69	4.06	110.34	5.45	12.07	169.31	5.77	389.66	3.05	220.35
300	8.97	337.09	4.27	163.54	4.24	12.06	162.91	5.43	336.46	3.02	173.55
400	9.21	343.56	4.75	211.36	3.02	12.05	156.44	5.23	288.64	3.01	132.20
500	9.45	349.85	5.48	250.47	1.73	12.04	150.15	5.13	249.53	3.00	99.38
600	9.69	355.77	6.34	281.02	0.41	12.03	144.23	5.08	218.98	3.00	74.75
631.47	***9.77***	***357.57***	***6.62***	***289.22***	***0.00***	***12.03***	***142.43***	***5.07***	***210.78***	***3.00***	***68.35***
700	9.77	357.57	6.62	289.22	0.00	12.03	142.43	5.07	210.78	3.00	68.35
800	9.77	357.57	6.62	289.22	0.00	12.03	142.43	5.07	210.78	3.00	68.35
900	9.77	357.57	6.62	289.22	0.00	12.03	142.43	5.07	210.78	3.00	68.35

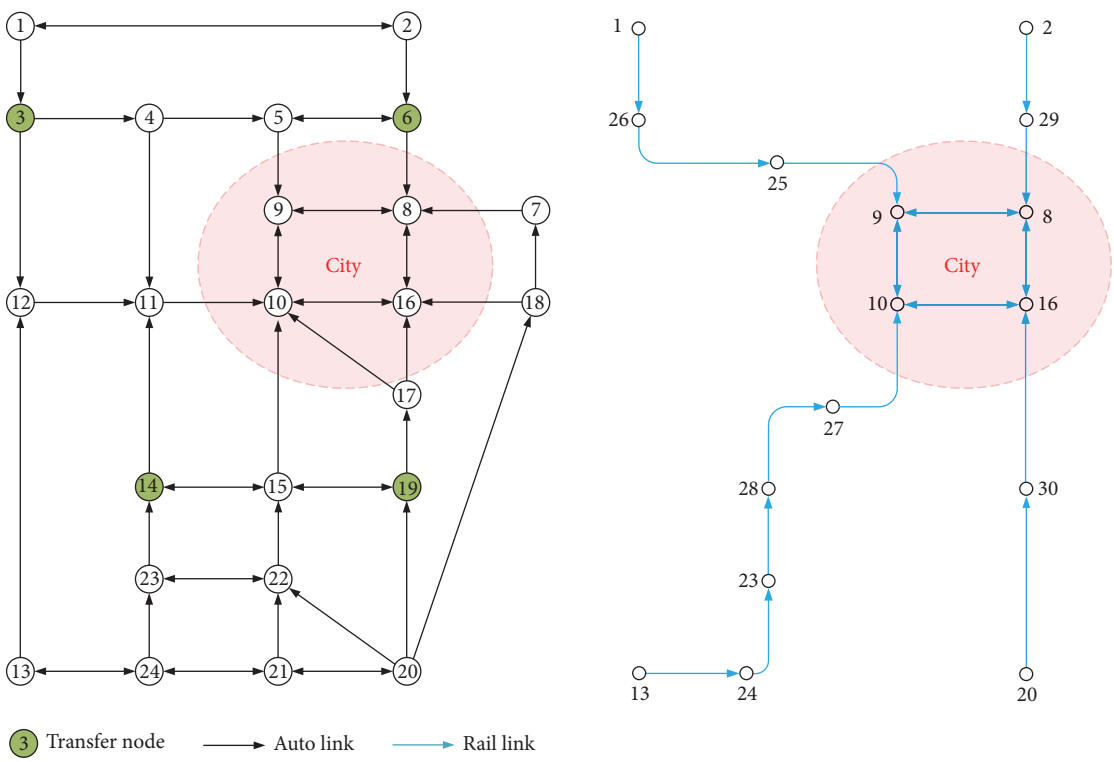

Figure 3: Modified Sioux-Falls network with RPR scheme.

influence travellers' mode choice as well as route choice behaviour. 14.03% of previous autodrivers and 5.51% of previous train riders shift to RPR mode, due to the utility provided by RPR services. The amount of emissions on critical links also significantly reduced with the provision of RPR schemes. This phenomenon indicates RPR schemes could alleviate the environmental deterioration by redistributing the flow and modal demand in the network and reflects the rationality of modelling users modal choice and route choice decisions in a combined model, i.e., CMSTA.

We proceed to exert environmental constraints on these critical links. Here, we consider five scenarios of the thresholds and summarize in Table 4. Parameters in the SAGP algorithm are set as follows: $\mu = 0.85$, $\delta = 0.8$, and $\alpha^{(0)} = 1.0$. In order to reflect the convergence trend of the SAGP algorithm apparently, we take the following logarithmic value of the maximum absolute error as a performance index, namely,

$$\varepsilon = \log_{10}\left(\max\left(\left\|T_a - g_a v_a\right\|_2, \forall a \in \overline{A}\right)\right) \tag{31}$$

The SAGP algorithm is then used to solve the environmental constrained CMSTA in terms of the five scenarios provided in Table 4. Figure 5 depicts the logarithmic value of the maximum absolute error versus the number of iterations used for solving scenarios 1, 2, 3, and 4. It clearly shows that the

Table 4: Five scenarios of environmental constraints.

Link ID	Scenario 1 Threshold T_a^1	Scenario 2 Threshold T_a^2	Scenario 3 Threshold T_a^3	Scenario 4 Threshold T_a^4	Scenario 5 Threshold T_a^5	Emission	Link flow
14	500	600	700	800	900	724.16	320.28
22	500	600	700	800	900	1007.05	370.93
29	500	600	700	800	900	796.13	319.51
46	500	600	700	800	900	866.88	351.1
48	500	600	700	800	900	735.61	531.39

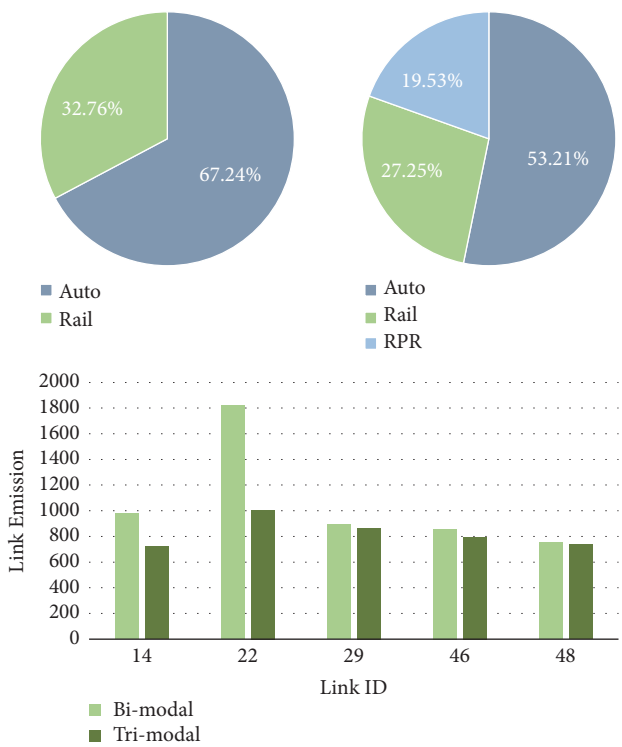

Figure 4: Mode share and emissions with/without RPR scheme.

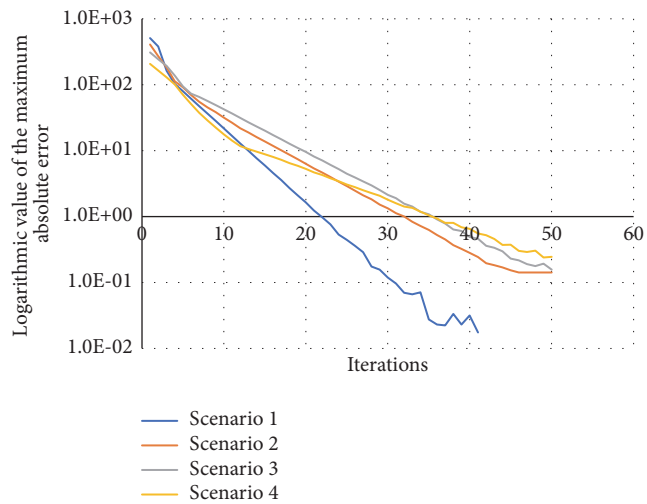

Figure 5: Convergence trend of the SAGP algorithm.

algorithm can converge to a solution of VI model $VI(\mathbf{g}, \overline{\Omega})$. In scenario 5, the solution converges much faster than other scenarios because only link 22 is constrained.

Table 5 gives the resultant link emissions and corresponding Lagrangian multiplier for each scenario. We can observe that the emissions on each link are bounded by the required thresholds (some link emissions slightly excess the requirements caused by the computation error). The corresponding multiplier takes positive value only on the links with emission bounded by the threshold. These two phenomena tally with (16)-(18), which numerically verify the effectiveness of the VI model $VI(\mathbf{g}, \overline{\Omega})$ and the SAGP algorithm. In addition, from scenario 1 to scenario 5, it can be seen that, by tightening the thresholds, the corresponding Lagrangian multipliers become larger, which indicates that it would be more costly to restrict the emission to a much lower level.

Table 6 further investigates the modal shift trend from scenario 1 to scenario 5. As the values of threshold getting smaller, travellers who use automode become less. The environmental regulations in road network could significantly promote the modal shift from auto to "green" travel modes (i.e., Train and RPR). Taking scenario 1, for example, the automode share is depressed about 11.11%, from 53.21% to 42.10%, where 5.38% of travel demand shifts to rail mode and 5.72% rest shifts to RPR mode. This phenomenon indicates that environmental regulations significantly influence not only travellers' route choice behaviour but also mode choice behaviour.

To further see the impacts of demand level on the Lagrangian multipliers, a sensitivity test is carried out on the dispersion parameter on the modal choice function (8). Without loss of generality, the first scenario of threshold setting is taken for this test, and then the value of θ is changed from 0.5 to 0.9 with an interval of 0.1. The Lagrangian multipliers obtained by the SAGP algorithm in these five cases are presented in Table 7. We noted that a larger value of θ results in a larger level of autodemand level and the road network congestion level is higher accordingly. Table 7 indicates the generalized CMSTA conditions can still be fulfilled. As the demand level ascends, the corresponding Lagrangian multipliers also increases, meaning that it is more difficult to maintain the threshold constraints at a higher demand level.

We further compare the network-level performance before and after implementing the set of environmental

Table 5: Link emission and corresponding Lagrangian multiplier.

Link ID	Scenario 1		Scenario 2		Scenario 3		Scenario 4		Scenario 5		Without
	Emission	LM	Emission	LM	Emission	LM	Emission	LM	Emission	LM	
14	499.99	1.64	600.06	0.93	700.07	0.22	728.78	0.00	726.51	0.00	724.16
22	500.00	2.29	600.03	1.74	700.10	1.20	800.17	0.64	900.00	0.38	1007.05
29	500.00	0.79	600.00	0.23	700.03	0.10	800.06	0.03	867.92	0.00	866.88
46	500.02	2.32	600.14	1.5	700.09	0.77	800.21	0.15	803.76	0.00	796.13
48	500.03	0.86	600.02	0.71	699.99	0.32	743.59	0.00	736.09	0.00	735.61

∗LM denotes Lagrangian multiplier.

Table 6: Mode share with different threshold levels.

Mode	With Threshold					Without Threshold
	Scenario 1	Scenario 2	Scenario 3	Scenario 4	Scenario 5	
Auto	42.10%	45.68%	48.96%	51.53%	52.35%	53.21%
Train	32.64%	30.64%	28.89%	27.61%	27.39%	27.25%
RPR	25.26%	23.68%	22.15%	20.86%	20.27%	19.53%

Table 7: Sensitivity test on the dispersion parameter.

link ID	$\theta = 0.5$		$\theta = 0.6$		$\theta = 0.7$		$\theta = 0.8$		$\theta = 0.9$	
	Emission	LM	Emission	LM	Emission	LM	Emission	LM	Emission	LM
14	499.99	1.64	500.00	1.70	499.98	1.73	500.01	1.74	500.02	1.75
22	500.00	2.29	500.00	2.02	500.00	1.82	500.02	1.66	500.01	1.54
29	500.00	0.79	500.01	0.68	500.01	0.59	500.00	0.52	500.01	0.48
46	500.02	2.32	500.03	2.38	500.03	2.41	500.00	2.42	500.06	2.43
48	500.03	0.86	500.01	0.85	499.94	0.84	500.02	0.84	499.96	0.83

∗LM denotes Lagrangian multiplier.

restraints. The first scenario of threshold setting is still taken for this test. Without loss of generality, the total travel time (TTT) and total vehicle distances (TVD) travelled are used in this study to measure the network-wide performance. From Table 8 we can observe that implementation of environmental constraints decreases both TTT and TVD (-13.89% decrease of TTT and -13.19% decrease of TVM), which implies that some travellers must be shifting their modes in order to benefit the air quality of the CBD area.

7. Conclusions

Environmental protection is an important consideration in planning a transportation system. Environmental constraint is a useful means to explicitly reflect environmental protection requirements. In this paper, we studied a combined environmental protection strategy in the multimodal transport network: (1) a rail-based park-and-ride scheme to assist mode shift to reduce the overall vehicle travel demands in the road network and (2) an area-based regulation scheme to deal with the environmental deterioration caused by heterogeneity of traffic flows. To quantitatively evaluate the effectiveness of the proposed scheme, we built an environmental constrained combined modal split and traffic assignment (EC-CMSTA) model. Specifically, we developed an equivalent VI reformulation for the EC-CMSTA. Different from the explicit formulation as a VI or NCP, the proposed reformulation adapts the concept of fix-point to reformulate the CMSTA conditions, which is, later, incorporated into the VI formulated nonlinear complementarity conditions associated with the nonlinear environmental constraints. The proposed VI reformulation can handle a general nonlinear environmental constraint structure and a general link and route cost structure, enhancing the modelling adaptability and flexibility, and in addition permits a number of efficient algorithms for its solution. A customized projection algorithm with self-adaptive step size scheme is adopted in this paper. Numerical examples demonstrated the EC-CMSTA model has the potential to enhance the behavioural modelling of network users' travel decisions and to assist in quantitatively evaluating the effectiveness of RPR schemes and environmental regulations.

Several directions are worthy of further investigation. First, in this paper, we use CO as an indicator to model vehicle emission. Further study will take other types of emission into consideration, e.g., the CO_2. Second, a number of efficient solution algorithms proposed by recent studies, e.g., Ryu, Chen, and Choi [34]; Ryu, Chen, and Choi [40], should be explored to further improve the solution efficiency. Third, we plan to test our model on larger networks with more real world applications. For very large-scale problems, existing algorithms may be not efficient and specific algorithms should be developed.

Table 8: Network performance with and without environmental regulations.

Network performance	Without environmental Regulation (a)	With environmental regulation (b)	Relative difference [(b-a)/a]
Total travel time	41442.50	35685.36	-13.89%
Total vehicle distance	38995.10	33851.32	-13.19%

Appendix

A. Proof of Proposition 5

Vector function $\mathbf{g}(\mathbf{u})$ is strictly monotone on $\overline{\Omega}$; namely,

$$\left(\mathbf{g}\left(\mathbf{u}'\right)-\mathbf{g}\left(\mathbf{u}''\right)\right)^T\left(\mathbf{u}'-\mathbf{u}''\right)>0,\quad \forall \mathbf{u}',\mathbf{u}''\in\overline{\Omega} \tag{A.1}$$

Proof. For any two distinct nonnegative Lagrangian multiplier vectors $\mathbf{u}'$ and $\mathbf{u}''$, let $\mathbf{v}(\mathbf{u}')$ and $\mathbf{v}(\mathbf{u}'')$ denote the corresponding CMSTA link flow solutions, and similarly, let $\mathbf{f}(\mathbf{u}')$, $\mathbf{f}(\mathbf{u}'')$, $\mathbf{q}(\mathbf{u}')$, and $\mathbf{q}(\mathbf{u}'')$ denote the corresponding CMSTA path flow and modal demand solutions. We have

$$\mathbf{v}\left(\mathbf{u}'\right)=\Delta\mathbf{f}\left(\mathbf{u}'\right) \tag{A.2}$$

$$\mathbf{v}\left(\mathbf{u}''\right)=\Delta\mathbf{f}\left(\mathbf{u}''\right) \tag{A.3}$$

$$\mathbf{f}\left(\mathbf{u}'\right)=\mathbf{q}\left(\boldsymbol{\tau}'\right)^T\cdot\mathbf{p}\left(\widehat{\mathbf{c}}'\right) \tag{A.4}$$

$$\mathbf{f}\left(\mathbf{u}''\right)=\mathbf{q}\left(\boldsymbol{\tau}''\right)^T\cdot\mathbf{p}\left(\widehat{\mathbf{c}}''\right) \tag{A.5}$$

$$\mathbf{q}\left(\widehat{\boldsymbol{\tau}}'\right)=\overline{\mathbf{q}}^T\cdot\overline{\mathbf{p}}\left(\widehat{\boldsymbol{\tau}}'\right) \tag{A.6}$$

$$\mathbf{q}\left(\widehat{\boldsymbol{\tau}}''\right)=\overline{\mathbf{q}}^T\cdot\overline{\mathbf{p}}\left(\widehat{\boldsymbol{\tau}}''\right) \tag{A.7}$$

where Δ defines the link-path incidence, $\widehat{\mathbf{c}}'=\Delta^T\widehat{\mathbf{t}}(\mathbf{v}(\mathbf{u}'),\mathbf{u}')$, $\widehat{\mathbf{c}}''=\Delta^T\widehat{\mathbf{t}}(\mathbf{v}(\mathbf{u}''),\mathbf{u}'')$, $\mathbf{p}(\widehat{\mathbf{c}}')=(p_k^{m,od}(\widehat{\mathbf{c}}'),\ \forall k\in K_m^{od},\ m\in M_{od},\ od\in W)^T$, $\mathbf{p}(\widehat{\mathbf{c}}'')=(p_k^{m,od}(\widehat{\mathbf{c}}''),\ \forall k\in K_m^{od},\ m\in M_{od},\ od\in W)^T$, $\widehat{\boldsymbol{\tau}}'=(\tau_m'^{od}(\widehat{\mathbf{c}}'),\ \forall m\in M_{od},\ od\in W)^T$, $\widehat{\boldsymbol{\tau}}''=(\widehat{\tau}_m''^{od}(\widehat{\mathbf{c}}''),\ \forall m\in M_{od},\ od\in W)^T$, $\overline{\mathbf{p}}(\widehat{\boldsymbol{\tau}}')=(p_m^{od}(\widehat{\boldsymbol{\tau}}'),\ \forall m\in M_{od},\ od\in W)^T$, $\overline{\mathbf{p}}(\widehat{\boldsymbol{\tau}}'')=(p_m^{od}(\widehat{\boldsymbol{\tau}}''),\ \forall m\in M_{od},\ od\in W)^T$, and $\overline{\mathbf{q}}=(\overline{q}^{od},\ \forall od\in W)^T$.

According to the definition of CMSTA conditions, the modal travel time τ_m^{od} is taken as the equilibrium path travel time of mode m, it follows that

$$\tau_m^{od}\le c_k^{m,od},\quad \forall k\in K_m^{od}; \tag{A.8}$$

together with the flow conservation condition (5), we have

$$\mathbf{q}\left(\boldsymbol{\tau}'\right)^T\boldsymbol{\tau}'\le\mathbf{f}\left(\mathbf{u}'\right)^T\mathbf{c}' \tag{A.9}$$

$$\mathbf{q}\left(\boldsymbol{\tau}''\right)^T\boldsymbol{\tau}''\le\mathbf{f}\left(\mathbf{u}''\right)^T\mathbf{c}'' \tag{A.10}$$

Subtracting (A.9) and (A.10) yields that

$$\mathbf{q}\left(\boldsymbol{\tau}'\right)^T\left(\boldsymbol{\tau}'-\boldsymbol{\tau}''\right)\le\mathbf{f}\left(\mathbf{u}'\right)^T\left(\mathbf{c}'-\mathbf{c}''\right) \tag{A.11}$$

$$\mathbf{q}\left(\boldsymbol{\tau}''\right)^T\left(\boldsymbol{\tau}'-\boldsymbol{\tau}''\right)\le\mathbf{f}\left(\mathbf{u}''\right)^T\left(\mathbf{c}'-\mathbf{c}''\right); \tag{A.12}$$

namely,

$$\begin{aligned}&\left(\mathbf{q}\left(\boldsymbol{\tau}'\right)-\mathbf{q}\left(\boldsymbol{\tau}''\right)\right)^T\left(\boldsymbol{\tau}'-\boldsymbol{\tau}''\right)\\&\quad\le\left(\mathbf{f}\left(\mathbf{u}'\right)-\mathbf{f}\left(\mathbf{u}''\right)\right)^T\left(\mathbf{c}'-\mathbf{c}''\right)\end{aligned} \tag{A.13}$$

The monotonicity of function (8) implies that

$$\left(\mathbf{q}\left(\boldsymbol{\tau}'\right)-\mathbf{q}\left(\boldsymbol{\tau}''\right)\right)^T\left(\boldsymbol{\tau}'-\boldsymbol{\tau}''\right)>0 \tag{A.14}$$

According to (A.13) and (A.14), we thus obtain

$$\left(\mathbf{f}\left(\mathbf{u}'\right)-\mathbf{f}\left(\mathbf{u}''\right)\right)^T\left(\mathbf{c}'-\mathbf{c}''\right)>0 \tag{A.15}$$

As $\mathbf{c}'=\Delta^T\widehat{\mathbf{t}}(\mathbf{v}(\mathbf{u}'),\mathbf{u}')$ and $\widehat{\mathbf{c}}''=\Delta^T\widehat{\mathbf{t}}(\mathbf{v}(\mathbf{u}''),\mathbf{u}'')$, (A.15) can be equivalently written as

$$\begin{aligned}&\left(\mathbf{f}\left(\mathbf{u}'\right)-\mathbf{f}\left(\mathbf{u}''\right)\right)^T\\&\quad\cdot\left(\Delta^T\widehat{\mathbf{t}}\left(\mathbf{v}\left(\mathbf{u}'\right),\mathbf{u}'\right)-\Delta^T\widehat{\mathbf{t}}\left(\mathbf{v}\left(\mathbf{u}''\right),\mathbf{u}''\right)\right)>0\end{aligned} \tag{A.16}$$

Rearranging the left side of (A.16), it follows that

$$\begin{aligned}&\left(\mathbf{v}\left(\mathbf{u}'\right)-\mathbf{v}\left(\mathbf{u}''\right)\right)^T\\&\quad\cdot\left(\Delta^T\widehat{\mathbf{t}}\left(\mathbf{v}\left(\mathbf{u}'\right),\mathbf{u}'\right)-\Delta^T\widehat{\mathbf{t}}\left(\mathbf{v}\left(\mathbf{u}''\right),\mathbf{u}''\right)\right)>0\end{aligned} \tag{A.17}$$

According to the definition of generalized link travel time function, (20), we have

$$\left(\mathbf{v}\left(\mathbf{u}'\right)-\mathbf{v}\left(\mathbf{u}''\right)\right)^T\left(\mathbf{u}'-\mathbf{u}''\right)>0 \tag{A.18}$$

Together with Assumption 1, $\mathbf{g}(\mathbf{u})$ is a strictly monotone function with respect to link flow solutions $\mathbf{v}(\mathbf{u})$; it follows that

$$\left(\mathbf{g}\left(\mathbf{u}'\right)-\mathbf{g}\left(\mathbf{u}''\right)\right)^T\left(\mathbf{u}'-\mathbf{u}''\right)>0 \tag{A.19}$$

which implies $\mathbf{g}(\mathbf{u})$ is strictly monotone with respect to $\mathbf{u}$ on $\overline{\Omega}$. □

B. Proof of Proposition 6

Vector function $\mathbf{g}(\mathbf{u})$ is Lipschitz continuous on $\overline{\Omega}$; namely,

$$\left\|\mathbf{g}\left(\mathbf{u}'\right)-\mathbf{g}\left(\mathbf{u}''\right)\right\|_2\le L\left\|\mathbf{u}'-\mathbf{u}''\right\|,\quad \forall \mathbf{u}',\mathbf{u}''\in\overline{\Omega} \tag{B.1}$$

Proof. Following the approach presented by Meng, Liu, and Wang [28], it is easily to conclude that $\mathbf{v}(\mathbf{u})$ is continuously differentiable in a neighbourhood of $\mathbf{u}_0$ according to the implicit function theorem [41].

Since $\mathbf{v}(\mathbf{u})$ is continuously differentiable on $\overline{\Omega}$, its Jacobian matrix $\nabla_{\mathbf{u}}\mathbf{v}(\mathbf{u})$ is thus continuous on $\overline{\Omega}$. The two-norm of $\nabla_{\mathbf{u}}\mathbf{v}(\mathbf{u})$ is therefore bounded from the nonempty closed and convex set $\overline{\Omega}$; namely, there is a positive constant such that

$$\left\|\nabla_{\mathbf{u}}\mathbf{v}\left(\mathbf{u}\right)\right\|_2\le L_1,\quad \forall \mathbf{u}\in\overline{\Omega} \tag{B.2}$$

According to the Theorem 3.2.4 of Ortega and Rheinboldt [41] (mean-value theorem), it can be seen that

$$\left\|\mathbf{v}\left(\mathbf{u}'\right)-\mathbf{v}\left(\mathbf{u}''\right)\right\|_2 \le L_1\left\|\mathbf{u}'-\mathbf{u}''\right\|_2, \quad \forall \mathbf{u}', \mathbf{u}'' \in \overline{\Omega} \tag{B.3}$$

Similarly, according to **Assumption 1**, $\mathbf{g}(\mathbf{v})$ is a continuous differentiable function w.r.t. $\mathbf{v}$. The Jacobian matrix $\nabla_{\mathbf{v}}\mathbf{g}(\mathbf{v})$ is thus continuous on Ω which is also nonempty closed and convex. Thus, there is a positive constant such that

$$\left\|\nabla_{\mathbf{v}}\mathbf{g}(\mathbf{v})\right\|_2 \le L_2, \quad \forall \mathbf{v} \in \Omega \tag{B.4}$$

and we have

$$\left\|\mathbf{g}\left(\mathbf{v}'\right)-\mathbf{g}\left(\mathbf{v}''\right)\right\|_2 \le L_2\left\|\mathbf{v}'-\mathbf{v}''\right\|_2, \quad \forall \mathbf{v}', \mathbf{v}'' \in \Omega \tag{B.5}$$

According to (B.3) and (B.5), we thus have

$$\begin{aligned}\left\|\mathbf{g}\left(\mathbf{u}'\right)-\mathbf{g}\left(\mathbf{u}''\right)\right\|_2 &\le L_2\left\|\mathbf{v}'-\mathbf{v}''\right\|_2 \\ &\le L_2 \cdot L_1\left\|\mathbf{u}'-\mathbf{u}''\right\|, \\ &\qquad \forall \mathbf{u}', \mathbf{u}'' \in \overline{\Omega}\end{aligned} \tag{B.6}$$

This completes the proof. □

C. Proof of Proposition 7

$\mathbf{u}^* = (u_a^*, \forall a \in E)$ is a solution of $VI(\mathbf{g}, \mathfrak{R}_+^{|E|})$ if and only if $\mathbf{u}^*$ and $\mathbf{v}(\mathbf{u}^*)$ fulfil the generalized CMSTA conditions (15)-(18).

Proof.

Necessary Condition. Suppose $\mathbf{u}^*$ is a solution of $VI(\mathbf{g}, \mathfrak{R}_+^{|E|})$, and we now show that $\mathbf{u}^*$ fulfil the generalized CMSTA conditions.

We first demonstrate that $u_a^* < \overline{M}, \forall a \in E$. Assume that there is at least on element $b \in E$ with $u_b^* = \overline{M}$. Then, we define a feasible vector $\mathbf{u}' \in \mathfrak{R}_+^{|E|}$.

$$\mathbf{u}' = \left(u_a' = u_a^*,\ \forall a \in E \setminus \{b\},\ u_b' = 0.5\overline{M}\right)^T. \tag{C.1}$$

Substituting $\mathbf{u}$ in the VI model $VI(\mathbf{g}, \mathfrak{R}_+^{|E|})$ with vector $\mathbf{u}'$, it follows that

$$\left(-g_b\left(v_b\left(\mathbf{u}^*\right)\right)\right) \cdot \left(0.5\overline{M}-\overline{M}\right) \ge 0; \tag{C.2}$$

namely,

$$g_b\left(v_b\left(\mathbf{u}^*\right)\right) \ge 0 \tag{C.3}$$

Now, we proceed to demonstrate $u_a^* < \overline{M}$, $\forall a \in E$ by using an apagogical approach. Note that, according to the monotony increasing of $\mathbf{g}(\mathbf{v})$, there exists a upper bound of link flow $\overline{v}_b$ that, for any flow $v_b < \overline{v}_b$, we have

$$g_b\left(v_b\left(\mathbf{u}^*\right)\right) < 0 \tag{C.4}$$

Then, we proceed to show $v_a(\mathbf{u}^*) < \overline{v}_a, \forall a \in E$. Suppose at least one flow loaded path on the road network uses link b. According to the DUE conditions, for any flow loaded paths, they have identical path travel time. Denote one of these paths as k_o and its $\lambda_{k_0}^{m,od}(\mathbf{u}^*)$ follows that

$$\lambda_{k_0}^{m,od}\left(\mathbf{u}^*\right) = \sum_{a\in E} u_a^* \zeta_{e,k_0}^{m,od} > \overline{M} \tag{C.5}$$

Therefore, its generalized path travel time and the corresponding modal travel time fulfil the condition:

$$c_{k_0}^{m,od}\left(\mathbf{u}^*\right) + \lambda_{k_0}^{m,od}\left(\mathbf{u}^*\right) > \overline{M} \tag{C.6}$$

$$c_m^{od}\left(\mathbf{u}^*\right) + \lambda_m^{od}\left(\mathbf{u}^*\right) \ge c_{k_0}^{m,od}\left(\mathbf{u}^*\right) + \lambda_{k_0}^{m,od}\left(\mathbf{u}^*\right) > \overline{M} \tag{C.7}$$

According to the monotonicity of function (8), we have

$$q_m^{od}\left(c_m^{od}\left(\mathbf{u}^*\right) + \lambda_m^{od}\left(\mathbf{u}^*\right)\right) \le q_m^{od}\left(\overline{M}\right) < \frac{\overline{v}_b}{|W| \cdot |M|} \tag{C.8}$$

In other words,

$$v_b < \sum_{od\in W}\sum_{m\in M_{od}} q_m^{od} < \overline{v}_b \tag{C.9}$$

$$g_b\left(v_b\left(\mathbf{u}^*\right)\right) < 0 \tag{C.10}$$

However, (C.10) contradicts (C.3), then the hypothesis $u_b^* = \overline{M}$ is incorrect. In other words,

$$u_a^* < \overline{M}, \quad \forall a \in E \tag{C.11}$$

To further prove the necessary conditions, we construct the following two specific vectors for any link $a \in E$:

$$\mathbf{u}' = \left(u_a' = (1-\gamma_1)u_a^* + \gamma_1\overline{M},\ \forall a \in E\right)^T \tag{C.12}$$

$$\mathbf{u}'' = \left(u_a'' = \gamma_1 u_a^*,\ \forall a \in E\right)^T \tag{C.13}$$

where $\gamma_1 \in (0,1)$ is a given parameter. Substituting vector $\mathbf{u}$ of VI model $VI(\mathbf{g}, \mathfrak{R}_+^{|E|})$ with these two particular vectors, respectively, yields that

$$g_a(\mathbf{v})\left(\gamma_1\left(\overline{M}-u_a^*\right)\right) \le 0 \tag{C.14}$$

$$g_a(\mathbf{v})\left((\gamma_1-1)u_a^*\right) \le 0 \tag{C.15}$$

Since $M - u_a^* > 0$, (C.14) implies that

$$g_a(\mathbf{v}) \le 0, \quad \forall a \in E \tag{C.16}$$

In accordance with the fact that $u_a^* \ge 0$, we thus have

$$\left(-g_a(\mathbf{v})\right) \cdot u_a^* \ge 0, \quad \forall a \in E \tag{C.17}$$

Hence, (C.17) in conjunction with (C.15) implies that

$$\left(-g_a(\mathbf{v})\right) \cdot u_a^* = 0, \quad \forall a \in E \tag{C.18}$$

In other words, $\mathbf{u}^*$ and $\mathbf{v}(\mathbf{u}^*)$ fulfil the generalized CMSTA conditions.

Sufficient Condition. Suppose $\mathbf{u}^*$ fulfil the generalized CMSTA conditions (15)-(18); we have the following conditions:

$$-\mathbf{g}\left(\mathbf{v}\left(\mathbf{u}^*\right)\right) \ge \mathbf{0} \tag{C.19}$$

$$\mathbf{g}\left(\mathbf{v}\left(\mathbf{u}^*\right)\right)^T \cdot \mathbf{u}^* = 0 \tag{C.20}$$

In addition, we have $\mathbf{u} \ge 0$. Therefore, according to (C.19) and (C.20), it follows that

$$\mathbf{g}\left(\mathbf{v}\left(\mathbf{u}^*\right)\right)^T \cdot \mathbf{u} \ge \mathbf{g}\left(\mathbf{v}\left(\mathbf{u}^*\right)\right)^T \cdot \mathbf{u}^* \tag{C.21}$$

$$\mathbf{g}\left(\mathbf{v}\left(\mathbf{u}^*\right)\right)^T \cdot \left(\mathbf{u}-\mathbf{u}^*\right) \ge 0 \tag{C.22}$$

This completes the proof. □

Table 9

ID	T	H	Fft	Capa	Type
1	8	9	3	400	Auto
2	9	8	3	400	Auto
3	9	10	3	400	Auto
4	10	9	3	400	Auto
5	10	16	3	400	Auto
6	16	10	3	400	Auto
7	8	16	3	400	Auto
8	16	8	3	400	Auto
9	1	3	3	800	Auto
10	3	4	4	1200	Auto
11	4	3	4	1200	Auto
12	4	5	5	800	Auto
13	5	4	5	800	Auto
14	5	9	5	800	Auto
15	1	2	8	600	Auto
16	3	12	6	1200	Auto
17	4	11	7	600	Auto
18	5	6	3	800	Auto
19	6	5	3	800	Auto
20	12	11	5	600	Auto
21	2	6	3	800	Auto
22	6	8	6	800	Auto
23	2	1	8	600	Auto
24	13	24	3	600	Auto
25	24	23	4	600	Auto
26	23	14	4	600	Auto
27	14	15	3	1200	Auto
28	15	14	3	800	Auto
29	15	10	6	800	Auto
30	13	12	7	800	Auto
31	24	21	3	600	Auto
32	21	24	3	600	Auto
33	23	22	3	600	Auto
34	22	23	3	600	Auto
35	21	22	4	600	Auto
36	22	15	4	800	Auto
37	21	20	3	600	Auto
38	20	19	5	600	Auto
39	19	17	3	1200	Auto
40	17	16	3	600	Auto
41	17	10	5	400	Auto
42	20	22	3	400	Auto
43	15	19	3	600	Auto
44	7	8	3	400	Auto
45	19	15	3	600	Auto
46	11	10	5	600	Auto
47	14	11	4	400	Auto
48	18	16	3	600	Auto
49	18	7	4	600	Auto
50	20	21	3	600	Auto
51	20	18	7	600	Auto
52	24	13	3	600	Auto
53	9	10	3	1500	Train
54	9	8	3	1500	Train
55	10	9	3	1500	Train
56	10	16	3	1500	Train

Table 9: Continued.

ID	T	H	Fft	Capa	Type
57	8	9	3	1500	Train
58	8	16	3	1500	Train
59	16	10	3	1500	Train
60	16	8	3	1500	Train
61	20	30	7	1000	Train
62	30	16	6	1000	Train
63	13	24	2	1000	Train
64	24	23	4	1000	Train
65	23	28	4	1000	Train
66	28	27	4	1000	Train
67	27	10	4	1000	Train
68	2	29	10	1000	Train
69	29	8	2	1000	Train
70	1	26	3	1000	Train
71	26	25	9	1000	Train
72	25	9	7	1000	Train
73	3	26	4	1000	RPR
74	6	29	4	1000	RPR
75	14	28	3	1000	RPR
76	19	30	3	1000	RPR

∗T is tail node; H is head node; Fft denotes free flow time; Capa denotes capacity.

Table 10

ID	Origin	Destination	Demand
1	1	8	220
2	1	9	180
3	1	10	200
4	1	16	220
5	2	8	240
6	2	9	190
7	2	10	180
8	2	16	180
9	13	8	160
10	13	9	130
11	13	10	170
12	13	16	130
13	24	8	140
14	24	9	150
15	24	10	140
16	24	16	100
17	23	8	130
18	23	9	150
19	23	10	150
20	23	16	170
21	20	8	180
22	20	9	160
23	20	10	140
24	20	16	170

D. Attributes of Study Network

See Table 9.

E. OD Travel Demand of Study Network

See Table 10.

Data Availability

No data were used to support this study.

Conflicts of Interest

The authors declare that they have no conflicts of interest.

References

[1] X. Xu, A. Chen, and L. Cheng, "Reformulating environmentally constrained traffic equilibrium via a smooth gap function," *International Journal of Sustainable Transportation*, vol. 9, no. 6, pp. 419–430, 2015.

[2] S. Kitthamkesorn, A. Chen, X. Xu, and S. Ryu, "Modeling mode and route similarities in network equilibrium problem with go-green modes," *Networks and Spatial Economics*, vol. 16, no. 1, pp. 33–60, 2016.

[3] W. Y. Szeto, X. Jaber, and S. C. Wong, "Road network equilibrium approaches to environmental sustainability," *Transport Reviews*, vol. 32, no. 4, pp. 491–518, 2012.

[4] X. Chen, Z. Liu, I. Kim, and J. Leng, "Optimal Sitting and Sizing of the Remote Park-and-Ride Scheme in the Multimodal Transport Network," in *Proceedings of the Transportation Research Board 97th Annual Meeting*, Washington DC, USA, 2018.

[5] Z. Liu and Q. Meng, "Bus-based park-and-ride system: a stochastic model on multimodal network with congestion pricing schemes," *International Journal of Systems Science*, vol. 45, no. 5, pp. 994–1006, 2014.

[6] C. E. Wallace, K. Courage, D. Reaves, Schoene. G., and G. Euler, TRANSYT-7F user's manual.In.

[7] L. R. Rilett and C. M. Benedek, "Traffic assignment under environmental and equity objectives," *Transportation Research Record*, no. 1443, pp. 92–99, 1994.

[8] C. M. Benedek and L. R. Rilett, "Equitable traffic assignment with environmental cost functions," *Journal of Transportation Engineering*, vol. 124, no. 1, pp. 16–22, 1998.

[9] S. Sugawara and D. Niemeier, "How much can vehicle emissions be reduced? Exploratory analysis of an upper boundary using an emissions-optimized trip assignment," *Transportation Research Record Journal of the Transportation Research Board*, no. 1815, pp. 29–37, 2002.

[10] A. Chen, Z. Zhou, and S. Ryu, "Modeling physical and environmental side constraints in traffic equilibrium problem," *International Journal of Sustainable Transportation*, vol. 5, no. 3, pp. 172–197, 2011.

[11] Z.-C. Li, W. H. K. Lam, S. C. Wong, and A. Sumalee, "Environmentally sustainable toll design for congested road networks with uncertain demand," *International Journal of Sustainable Transportation*, vol. 6, no. 3, pp. 127–155, 2012.

[12] A. Nagurney, P. Ramanujam, and K. K. Dhanda, "A multimodal traffic network equilibrium model with emission pollution permits: complicance vs noncompliance," *Transportation Research Part D: Transport and Environment*, vol. 3, no. 5, pp. 349–374, 1998.

[13] E. Fernandez, J. de Cea, M. Florian, and E. Cabrera, "Network equilibrium models with combined modes," *Transportation Science*, vol. 28, no. 3, pp. 182–192, 1994.

[14] R. García and A. Marín, "Network equilibrium with combined modes: models and solution algorithms," *Transportation Research Part B: Methodological*, vol. 39, no. 3, pp. 223–254, 2005.

[15] Z.-C. Li, W. H. K. Lam, S. C. Wong, D.-L. Zhu, and H.-J. Huang, "Modeling park-and-ride services in a multimodal transport network with elastic demand," *Transportation Research Record: Journal of the Transportation Research Board*, no. 1994, pp. 101–109, 2007.

[16] W. H. Lam, Z. Li, S. C. Wong, and D. Zhu, "Modeling an elastic-demand bimodal transport network with park-and-ride trips," *Tsinghua Science and Technology*, vol. 12, no. 2, pp. 158–166, 2007.

[17] C. Pineda, C. E. Cortés, P. Jara-Moroni, and E. Moreno, "Integrated traffic-transit stochastic equilibrium model with park-and-ride facilities," *Transportation Research Part C: Emerging Technologies*, vol. 71, pp. 86–107, 2016.

[18] Z. Song, Y. He, and L. Zhang, "Integrated planning of park-and-ride facilities and transit service," *Transportation Research Part C: Emerging Technologies*, vol. 74, pp. 182–195, 2017.

[19] S. Kitthamkesorn and A. Chen, "Alternate weibit-based model for assessing green transport systems with combined mode and route travel choices," *Transportation Research Part B: Methodological*, vol. 103, pp. 291–310, 2017.

[20] Z. Liu, X. Chen, Q. Meng, and I. Kim, "Remote park-and-ride network equilibrium model and its applications," *Transportation Research Part B: Methodological*, vol. 117, pp. 37–62, 2018.

[21] S. Wang, Q. Meng, and H. Yang, "Global optimization methods for the discrete network design problem," *Transportation Research Part B: Methodological*, vol. 50, pp. 42–60, 2013.

[22] Z. Liu, S. Wang, and Q. Meng, "Optimal joint distance and time toll for cordon-based congestion pricing," *Transportation Research Part B: Methodological*, vol. 69, pp. 81–97, 2014.

[23] T. Liu, H. Huang, H. Yang, and X. Zhang, "Continuum modeling of park-and-ride services in a linear monocentric city with deterministic mode choice," *Transportation Research Part B: Methodological*, vol. 43, no. 6, pp. 692–707, 2009.

[24] D. Z. W. Wang and B. Du, "Reliability-based modeling of park-and-ride service on linear travel corridor," *Transportation Research Record: Journal of the Transportation Research Board*, vol. 2333, pp. 16–26, 2013.

[25] B. Du and D. Z. W. Wang, "Continuum modeling of park-and-ride services considering travel time reliability and heterogeneous commuters – A linear complementarity system approach," *Transportation Research Part E: Logistics and Transportation Review*, vol. 71, no. 0, pp. 58–81, 2014.

[26] Z. Liu, Q. Meng, and S. Wang, "Variational inequality model for cordon-based congestion pricing under side constrained stochastic user equilibrium conditions," *Transportmetrica A: Transport Science*, vol. 10, no. 8, pp. 693–704, 2014.

[27] T. Larsson and M. Patriksson, "Side constrained traffic equilibrium models— analysis, computation and applications," *Transportation Research Part B: Methodological*, vol. 33, no. 4, pp. 233–264, 1999.

[28] Q. Meng, Z. Liu, and S. Wang, "Asymmetric stochastic user equilibrium problem with elastic demand and link capacity constraints," *Transportmetrica A: Transport Science*, vol. 10, no. 4, pp. 304–326, 2014.

[29] C. F. Daganzo, "Stochastic network equilibrium with multiple vehicle types and asymmetric, indefinite link cost Jacobians," *Transportation Science*, vol. 17, no. 3, pp. 282–300, 1983.

[30] G. E. Cantarella, "A general fixed-point approach to multimode multi-user equilibrium assignment with elastic demand," *Transportation Science*, vol. 31, no. 2, pp. 107–128, 1997.

[31] A. Chen, X. Xu, S. Ryu, and Z. Zhou, "A self-adaptive Armijo stepsize strategy with application to traffic assignment models

and algorithms," *Transportmetrica A: Transport Science*, vol. 9, no. 8, pp. 695–712, 2011.

[32] A. Chen, Z. Zhou, and X. Xu, "A self-adaptive gradient projection algorithm for the nonadditive traffic equilibrium problem," *Computers & Operations Research*, vol. 39, no. 2, pp. 127–138, 2012.

[33] Z. Zhou, A. Chen, and S. C. Wong, "Alternative formulations of a combined trip generation, trip distribution, modal split, and trip assignment model," *European Journal of Operational Research*, vol. 198, no. 1, pp. 129–138, 2009.

[34] S. Ryu, A. Chen, and K. Choi, "Solving the combined modal split and traffic assignment problem with two types of transit impedance function," *European Journal of Operational Research*, vol. 257, no. 3, pp. 870–880, 2017.

[35] B. S. He, H. Yang, Q. Meng, and D. R. Han, "Modified Goldstein-Levitin-Polyak projection method for asymmetric strongly monotone variational inequalities," *Journal of Optimization Theory and Applications*, vol. 112, no. 1, pp. 129–143, 2002.

[36] D. Han and W. Sun, "A new modified Goldstein-Levitin-Polyakprojection method for variational inequality problems," *Computers Mathematics with Applications*, vol. 47, no. 12, pp. 1817–1825, 2004.

[37] Y. Yin and S. Lawphongpanich, "Internalizing emission externality on road networks," *Transportation Research Part D: Transport and Environment*, vol. 11, no. 4, pp. 292–301, 2006.

[38] A. Nagurney, Q. Qiang, and L. S. Nagurney, "Environmental impact assessment of transportation networks with degradable links in an era of climate change," *International Journal of Sustainable Transportation*, vol. 4, no. 3, pp. 154–171, 2010.

[39] X. Yang, X. J. Ban, and R. Ma, "Mixed equilibria with common constraints on transportation networks," *Networks and Spatial Economics*, vol. 17, no. 2, pp. 547–579, 2017.

[40] S. Ryu, A. Chen, and K. Choi, "Solving the stochastic multi-class traffic assignment problem with asymmetric interactions, route overlapping, and vehicle restrictions," *Journal of Advanced Transportation*, vol. 50, no. 2, pp. 255–270, 2016.

[41] J. M. Ortega and W. C. Rheinboldt, *Iterative Solution of Nonlinear Equations in Several Variables*, Academic Press, Thailand, 1970.